Assessment Of Driving Stress Through SVM And KNN Classifiers On Multi-Domain Physiological Data

Damiano Fruet
Department of Industrial Engineering
University of Trento
Trento, Italy
damiano.fruet@unitn.it

Chiara Barà
Department of Engineering
University of Palermo
Palermo, Italy
chiara.bara@community.unipa.it

Riccardo Pernice
Department of Engineering
University of Palermo
Palermo, Italy
riccardo.pernice@unipa.it

Luca Faes
Department of Engineering
University of Palermo
Palermo, Italy
luca.faes@unipa.it

Giandomenico Nollo
Department of Industrial Engineering
University of Trento
Trento, Italy
giandomenico.nollo@unitn.it

***Abstract*— We propose an objective stress assessment method based on the extraction of features from physiological time series and their classification using Support Vector Machine and K-Nearest Neighbors algorithms. For this purpose, we used an open dataset consisting of multiparametric physiological signals (electrocardiogram, electromyogram, galvanic skin response and breath signal) obtained during the execution of a driving route within the city of Boston with restful, highway and city driving periods indicative of three different stress states. To predict the driver stress level, 21 features were extracted from 122 chunks of raw signals and were subsequently managed by classification algorithms. Our analysis showed a prediction accuracy of 98.4% when all features were used, decreasing when signals from specific physiological systems were not considered. Our results highlighted that multidomain data acquisition by wearable sensors combined with appropriate classification models may represent a promising strategy to detect drivers' stress status in an unobtrusive and objective way that can in perspective be applicable in several other fields such as in the clinics.**

Keywords—Driving stress, Classification, Support Vector Machine, K-Nearest Neighbors, Electrocardiogram, Electromyogram, breath, Galvanic Skin Response

I. INTRODUCTION

Mental stress is an indirect physiological indicator of various diseases such as hyperextension, sleep disturbances or heart rhythm disorders. Stress-related conditions may seriously affect the quality of life of an individual by influencing the mood, behavior and health. Stress assessment is a procedure mainly carried out through visual evaluation [1] or questionnaires linked to predefined stress scales [2]. In this perspective, contrary to what happens for many clinical evaluations (e.g., magnetic resonance, ultrasonography, x-rays), stress assessment does not require any sophisticated technological tool, but results in a subjective and time-consuming evaluation.

Thanks to the many wearable devices available, nowadays it is possible to collect physiological information from different body districts in an unobtrusive and accurate way. Interestingly, the correct interpretation of such physiological information can lead to an objective evaluation of the stress level if appropriate features are used [3].

The aim of this study is to apply advanced signal processing techniques and classification algorithms to different physiological signals, to design a novel algorithmic approach to detect stress in an objective and efficient way. Several studies have exploited physiological signals to evaluate the stress while the user performs different tasks. Many of them exploit information from one physiological signal, such as the electrocardiogram (ECG) [4], the electromyogram (EMG) [5], or the skin conductance signal to detect stress in different experiments and conditions [6]. Other approaches focused on studying the combination of pairs of signals to evaluate the stress, such as ECG and EEG features [7] or blood pressure and heart rate to detect the stress during work [8]. Fully multiparametric approaches exploiting features from several simultaneously collected physiological districts are less explored in the literature.

Our approach is based on the data collected by J.A. Healey and made freely available on physionet (https://physionet.org/content/drivedb/1.0.0/). Such data consist of multiple physiological signals acquired on drivers during different stress-related driving conditions: restful, highway and city. Specifically, our study presents a stress assessment technique based on multiple features extracted from different raw physiological signals, i.e. ECG, EMG, respiratory, electrodermal activity (from hand and foot). After the first phase of feature extraction from raw signals, a classification step with Support Vector Machine (SVM) and K-Nearest Neighbors (KNN) algorithms was implemented to categorize the stress level. The SVM algorithm was already used for stress detection in studies starting from the EEG signal [9] or from both ECG and EMG, obtaining excellent results in terms of accuracy [10]. Other studies used the KNN algorithm for stress classification from the EEG signal [11] or the ECG signal [12]. In this work, SVM and KNN classifiers were compared, evaluating all the features from each signal or groups of them. Moreover, a data augmentation algorithm consisting in a sliding windows was implemented to increase the number of data points and thus increase the accuracy of the classifier.

Moreover, our study investigates how the different features extracted from physiological signals could train a classification algorithm able to determine stress status while driving. Compared with the study of Healey et al. [13], which

reported a stress detection methodology on the database we considered, our study aims at reaching an higher classification accuracy by using a data augmentation algorithm. In addition, the comparison between the SVM and K-NN classifiers on all the features and on selected physiological districts, may represent a promising strategy for an objective stress assessment and can open the way for future applications in different settings.

II. METHODS

A. Dataset description

The dataset used to extract features useful for the classification of a subject's stress state was collected in [13], [14] and consists of multiparametric acquisitions obtained during the execution of a driving route within the city of Boston, including restful, highway and city driving periods. Specifically, the dataset includes synchronous electrocardiogram (ECG), breath signal (BREATH), electromyogram (EMG) and foot and hand galvanic response of the skin (GSR) performed through a system integrated into the station wagon Volvo S70 used to perform the test. The acquisitions were made on 6 subjects who repeated the driving route several times and on 3 subjects who did it only once, for a total of 27 acquisitions. At the beginning and at the end of the experiment, the drivers underwent a resting phase, during which they were sitting in a garage with closed eyes and with the car in idle. Subsequently, the drivers exiting the garage crossed secondary roads until they reached the main busy roads of the city. Finally, there was a phase of driving on the highway. At the end of this route, the drivers turned back along the same route. Accordingly, each experiment consists of two rest phases (low stress), three city driving phases (high stress) and two highway driving phases (medium stress) for a total duration of 50-90 minutes. During acquisitions, the stress events to which the drivers were subjected were different (traffic, cyclists, pedestrians) and, in order to reduce variability, at the beginning of the experiment they were shown the route map and some rules; moreover, all the experiments were conducted in the mid-morning or mid-afternoon, in order to have a light traffic condition on the highway.

During the execution of the driving route, subjects were monitored by five sensors. The ECG signal was acquired through a modified lead II able to minimize motion artifacts and to maximize R peaks; specifically, the negative electrode was place near the base of the right clavicle, the positive one was place on a floating rib underneath the left armpit and the ground electrode was placed symmetrically to the latter. The breath signal activity was recorded through an elastic Hall effect sensor which, placed around the diaphragm of subjects, allowed to follow the movements due to inhalation and exhalation. Electromyography was performed using three electrodes placed on the right trapezius muscle. Finally, GSR signals on hands and feet were acquired via two electrodes placed on the middle segments of the first and middle finger on the side of the palm of the hand and on the sole of the foot at both ends of the arch of the foot, respectively. The sampling frequencies of the raw signals included in the database allowed an appropriate detection of the physiological dynamics (496 Hz for ECG, 31 Hz for BREATH, 15.5 Hz for EMG and 31 Hz for GSR). In all cases, the skin was cleaned by using alcohol and a conductive gel was applied between electrodes and skin.

In this work, nine acquisitions from 16 subjects were considered, as they are complete, including all the above-mentioned physiological signals and also the temporal information regarding the division of the driving phases.

B. Signal processing and features extraction

For each acquisition, the analyses were carried out on two windows of 300 consecutive heartbeats [15] for each driving phase, in order to consider the larger part of the signal for each participant. Specifically, 122 windows were selected considering all the subjects and the available driving phase data (32 windows at rest, 54 during city driving and 36 during highway driving). The first window was fixed at the beginning of each driving phase while the second was shifted 60 heartbeats from the start of the first. An example of windows selection for a subject is shown in Fig. 1 (a).This method of analysis, implemented in order to improve the performance of classification algorithms by means of the data augmentation technique [16], made it possible to double the number of elements of the dataset.

After the application of a zero-phase passband Butterworth filter (cutoff frequencies, cf_{HP} = 0.1 Hz cf_{LP} = 20 Hz, 4th order) on ECG signals, a modified version of Pan Tompkins algorithm was applied to detect R peaks [17], and the RR interval (RRI) time series were extracted as the time interval between consecutive R peaks. Starting from RRI time series, time-domain analysis was performed computing the average value (μ_{RR}), the standard deviation (σ_{RR}) and the root mean square of successive RRI interval differences ($RMSSD_{RR}$) used to estimate the vagally mediated changes reflected in HRV [15]. With regard to frequency-domain analysis, after applying a high-pass AR filter (cutoff at 0.0156 times the sampling rate) and normalizing the series to zero mean and unit variance, the power spectrum was obtained using the non-parametric Blackman-Tukey method (Hamming window, bandwidth of 0.04 Hz). After obtaining the RRI spectrum, low-frequency (*LF*, range 0.04-0.15 Hz) and high-frequency (*HF*, range 0.15-0.4 Hz) spectral power were computed to obtain their ratio (*LF/HF*) which is considered a pivotal index of the sympatho-vagal balance [15]. Fig. 1(b) reports exemplary RRI time series and power spectrum of ECG for a representative window.

With regard to breathing, after removing the mean value from the starting signal, a zero-phase bandpass Butterworth filter (cf_{HP} = 0.01 Hz cf_{LP} = 0.6 Hz, 4th order) was applied. In order to extract the time-domain indexes, the significant minima and maxima of the preprocessed signal were detected. Specifically, as significant peaks were considered the ones having a temporal distance greater than half of the average distance between all peaks and having an amplitude greater than half of the average amplitude; each minimum was detected as the smallest value between two consecutive significant peaks. Once the timing of maxima and minima were found, the respiratory rate (μ_{RESP}) and its variability (σ_{RESP}) were determined as the average and the standard deviation values of the inverse of the time distance between the maxima to which a 4-sample moving average filter was also applied. Moreover, the average inspiration (t_{INS}) and expiration (t_{ESP}) times were determined respectively as the average value of rise and fall times of the breathing signal in each respiratory act. Also in this case, after performing a subsampling of the signal at 2 Hz, the power spectrum was obtained using the Blackman-Tukey method (Hamming window, bandwidth of 0.04 Hz) and then the power value in

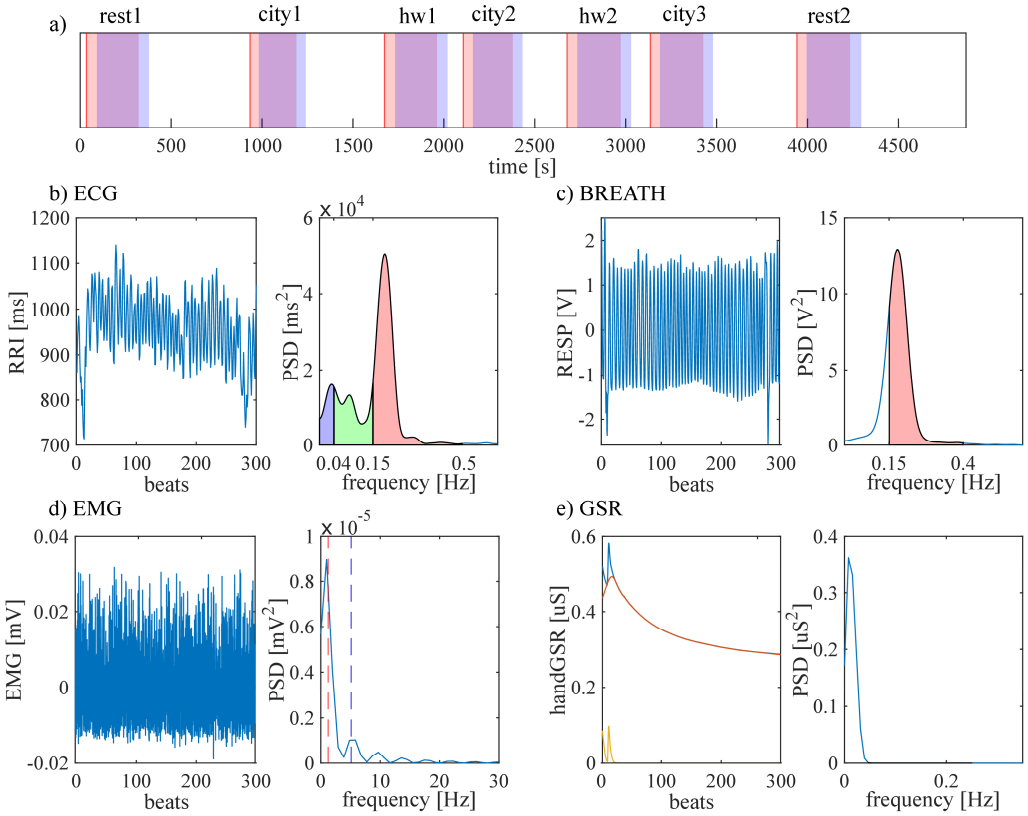

Fig. 1. Example of selected windows and relative physiological signals for one subject a) Graphical representation of the selected windows during the entire acquisition process. Above each pair of windows is indicated the driving condition (rest: restful driving, hw: driving on the highway, city: driving in the city). In red are represented the first windows consisting of 300 consecutive heartbeats, in blue the second window shifted of 60 heartbeats from the start of the first b-c-d-e) Example of time and frequency domain representation of physiological signals (b: ECG, c: BREATH, d: EMG, e: GSR) related to a single window.

the HF band (HF_{RESP}, range 0.15-0.4 Hz) was extracted. An example of breathing signal and of its power spectrum for a subject and in a window are reported in Fig. 1(c).

For the analysis of the muscle electrical activity, before extracting the parameters from the EMG signal, a preprocessing pipeline was applied as follows. The raw EMG signal was filtered with a zero-phase high pass Butterworth filter (cf = 10 Hz, 4th order), then it was rectified and smoothed using a zero-phase low pass Butterworth filter (cf = 5 Hz, 4th order) and, finally, normalized with respect to the average [18], [19]. From the preprocessed signals, the average rectified value (*ARV*) and the root mean square (*RMS*) were obtained as average of EMG absolute values and as the square root of the total power contained within the EMG signal [20]. With regard to frequency-domain analysis, after obtaining the power spectrum using the periodogram method [21], the mean (*MNF*) and the median (*MDF*) frequencies were used as indexes of muscle fatigue [20]. These two measures were extracted from 250 ms-long time windows [21], and then the indexes obtained for all the consecutive segments present within the 300 heartbeats were averaged. An example of EMG signal and its power spectrum are shown in Fig. 1(d).

The GSR signals acquired from hand and foot were preprocessed to extract physiological indexes as follows. The signal was subsampled at 20 Hz, smoothed by applying a moving average filter across a 1 second window to reduce artifacts and then normalized [22]. Then, a convex-optimization-based EDA model (*cvxEDA*) was applied to decompose the signal into phasic (SCR) and tonic (SCL) response [23]. After applying a zero-phase low pass Butterworth filter (cf = 5 Hz divided by sampling rate of the data) on the SCR component, starting from the identification of the onsets and offsets of the signals (at 0.01 and 0 μS, respectively), significant peaks were detected as maxima within onset-offset interval with a duration of at least 1 second [22]. The mean value of SCL component (μ_{SCL}) and the number of peaks of the SCR component (N_{SCR}) were considered. Before frequency-domain analysis, the GSR signal was filtered with a zero-phase low pass Chebyshev Type I filter (cf = 0.8 Hz, 8th order), subsampled to 2 Hz and then filtered with a zero-phase high pass Butterworth filter (cf = 0.01 Hz, 8th order). Power spectrum of GSR signal was calculated using the Welch's periodogram method (Blackman window with length of 128 points, 50% data overlap) [24]. The GSR spectrum was obtained using windows of 2 minutes, and the percentage of power within the range 0.045-0.25 Hz (*EDASymp*) was obtained as average of several power value percentages. Fig. 1(e) shows the normalized GSR signal acquired on hand, alongside with its components and its power spectrum for representative window.

In summary, for each acquisition and for each window, 21 parameters were extracted: 6 from ECG (μ_{RR}, σ_{RR}, $RMSSD_{RR}$, *LF, HF, LF/HF*), 5 from RESP ($\mu_{RESP}, \sigma_{RESP}, t_{INS}, t_{ESP}$, HF_{RESP}), 4 from EMG (*ARV*, *RMS*, *MNF*, *MDF*) and 6 from GSR (μ_{SCL}, N_{SCR}, *EDASymp*, both for hand and foot).

C. Machine learning: classification

The features extracted from the signals were organized in a table of 122 rows (one for each element) and 21 columns (one for each feature) which, given as input to the built-in Classification Learner App of the MATLAB environment [25] together with a vector containing labels ('rest', 'city' and

'hw'), allowed to compare several classification algorithms in terms of accuracy, prediction time and training time. We focused our attention on two classifiers, the Support Vector Machine (*SVM*) and the K-Nearest Neighbors (*KNN*). The former allows to identify a separation hyperplane between the elements of different classes [26]; specifically, a *cubic SVM* for which polynomial kernel degree is fixed to 3 was applied. Instead, the latter attributes to each element the class most present among its k neighbors [27]; in our analysis, the neighbors were identified by means of the Euclidean distance and the hyperparameter k was fixed to 1 (*fine KNN*). Training of the classification algorithms was performed using the cross-validation technique [28], for which the classifier is trained as many times as the random partitions identified within the dataset and the final result is given by their average. In our analyses, the hyperparameter k indicative of the number of partitions (or folds) used was first set to 50 and then to 5. Subsequently, cubic SVM and fine KNN were evaluated on the features extracted from each physiological signal, to investigate the contribution given by each single signal to the classification. Finally, the performance of classifiers was evaluated by subtracting progressively the features obtained from the same physiological signal from the whole feature set, proceeding at each step to maintain maximum accuracy, until a single signal was left. In these cases, the hyperparameter k of cross-validation technique was set to 5. Given the random nature of the validation technique [28], all learning analyzes were performed five times, computing the average accuracy, prediction speed and training time.

III. Results and Discussion

Table I shows the results in terms of accuracy, prediction speed and training time obtained with the application of cubic SVM and fine KNN algorithms on the dataset of 122 elements characterized by 21 features. The classifier showing the best accuracy (98.4%) was the cubic SVM with the application of 50 folds for validation. Looking at the several tests performed in these conditions, it could be observed that the accuracy remained quite constant while the training times and the number of objects predicted in one second changed. By setting to 5 number of folds, the accuracy also varied across acquisitions. It is important to note that in each of the tests performed with the cubic SVM, the accuracy always remained above 96%, with an average of 97.54%. A high number of k partitions identified in the application of cross-validation led to a similar training set during the k training phases, therefore to a lower variability of results obtained not only between the k trainings, but also between the different tests performed on the same database [28]. The choice of the optimal number of folds for validation is not trivial and strongly depends on the variability and collinearity of the database [29].

Evident differences were observed in terms of the two parameters considered for evaluation of the performance. Indeed, using 5 folds rather than 50, the training times decreased ~7.7 times and the number of predicted elements per second increased ~8.4 times. This observation may be relevant for the implementation of learning algorithms for real-time stress classification on wearable devices or automotive control systems.

Another relevant observation can be made with regard to the comparison between the two classifiers taken into account. In fact, for both validation techniques, using the fine KNN rather than the cubic SVM reduced the accuracy of about 2.5% for k = 50 and 2.12% for k = 5, with training times and speed of prediction on average lower of 44.95% and greater of 21.3%, respectively. These advantages in terms of time may be ascribed to the fact that the KNN classifier is among those that take the name of "lazy learner", for which the training mechanism does not foresee learning a discriminative function of the classes [30].

Table II shows the average values of accuracy, prediction speed and training time obtained during the five tests performed considering separately only the features extracted from each physiological signal. The best performance was obtained with features extracted from the breathing signal and in particular using the fine KNN. For most of the physiological signals, the fine KNN led to higher or comparable accuracies than those obtained with the cubic SVM, in addition to the advantages already highlighted in terms of time; in fact, some studies highlighted how, when working with a reduced number of features, the KNN classifier allows to achieve a greater accuracy than the SVM [31].

Our results are in accordance with previous studies which found that the breath signal allows to obtain high classification performances for stress detection [32]. On the other hand, our results appear different with those found in literature with

TABLE I. Performance of cubic SVM and fine KNN classifiers in terms of accuracy, prediction speed and trainig time considering all features for five tests using two cross-validation approaches (k=50 and k=5). M= mean values of the five tests

		k = 50			**k = 5**		
		Accuracy (%)	***Prediction speed (obs/s)***	***Training time (s)***	***Accuracy (%)***	***Prediction speed (obs/s)***	***Training time (s)***
1	cubic SVM	98.4	310	4.045	98.4	1900	0.791
	fine KNN	95.9	370	2.223	95.1	2900	0.495
2	cubic SVM	98.4	290	4.981	97.5	3100	0.525
	fine KNN	95.9	330	3.390	97.5	4100	0.269
3	cubic SVM	98.4	340	4.172	96.7	2400	0.554
	fine KNN	95.9	380	2.250	95.1	3600	0.295
4	cubic SVM	98.4	330	4.450	98.4	2800	0.532
	fine KNN	95.9	390	2.465	94.3	3600	0.283
5	cubic SVM	98.4	330	4.642	96.7	3200	0.490
	fine KNN	95.9	440	1.96	95.1	4000	0.261
M	cubic SVM	98.4	320 ± 20	4.458 ± 0.37	97.54 ± 0.85	2680 ± 535.72	0.578 ± 0.12
	fine KNN	95.9	382 ± 39.62	2.454 ± 0.56	95.42 ± 1.21	3640 ± 472.23	0.321 ± 0.10

TABLE II. PERFORMANCE OF CUBIC SVM AND FINE KNN CLASSIFIERS IN TERMS OF AVERAGE ACCURACY, PREDICTION SPEED AND TRAINING SPEED, CONSIDERING SEPARATELY ONLY THE FEATURES EXTRACTED FROM EACH SIGNAL WITH CROSS VALIDATION K=5

	Accuracy (%)	*Prediction speed (obs/s)*	*Training time (s)*
ECG			
cubic SVM	67.7 ± 4.73	2920 ± 268.33	0.54 ± 0.05
fine KNN	67.38 ± 2.92	4540 ± 384.71	0.28 ± 0.05
EMG			
cubic SVM	64.62 ± 2.40	3120 ± 327.11	0.76 ± 0.05
fine KNN	70 ± 1.69	4740 ± 313.05	0.25 ± 0.01
RESP			
cubic SVM	76.06 ± 4.17	3180 ± 178.89	0.52 ± 0.07
fine KNN	87.36 ± 2.52	4500 ± 380.79	0.25 ± 0.02
handGSR			
cubic SVM	70.66 ± 1.43	3240 ± 207.36	0.71 ± 0.29
fine KNN	71.32 ± 3.07	4860 ± 541.30	0.27 ± 0.06
footGSR			
cubic SVM	64.92 ± 0.93	3340 ± 181.66	0.94 ± 0.25
fine KNN	64.26 ± 2.49	4840 ± 288.10	0.26 ± 0.02

regard to GSR or EMG signals. In fact, although our analyses showed how these two signals considered singularly led to lower accuracy in the classification of the stress state, some studies applied on the same database but with different classification algorithms reported accuracies of 95.83% for GSR signal [33] and of 96% using EMG signal [34]. This result can be explained not only by the choice of the classifier but also by the different features that are considered with respect to those chosen in our work and which are probably less effective for stress detection.

Fig. 2 reports results obtained by removing, from all the available features, those extracted from a specific signal chosen to keep the classification accuracy as high as possible; this was done for both cubic SVM (top panel) and fine KNN (bottom panel). In both cases, the best accuracy was obtained using all the five signals and decreased by subtracting the features from a given signal. This trend was particularly evident using the cubic SVM. It is noteworthy that for KNN the accuracy obtained reducing the number of features taken into account is higher than the SVM; this could still be attributed to the fact that the performances of this classifier are better if few features are used [31].

Comparing results reported by Table II and Fig. 2, it can be observed that the signal that, when considered separately, on average has a lower accuracy is not always the one that is subtracted from the totality of signals. This result is probably related to the curse of dimensionality for which, using higher dimensional data, the presence of redundant features may lead to lower accuracy and longer processing times [35]. To alleviate this problem, it is possible to apply approaches for features selection even within the same physiological signal.

These results highlight the potential of classifiers such as SVM, but even more of KNN, to distinguish different stress conditions by starting from signals acquired from multiple physiological districts, but also from a single one. The results obtained are relevant from the point of view of implementing stress detection algorithms on wearable devices or systems integrated within the car. Despite the advantages shown in the above results, one of the main limitations of the KNN

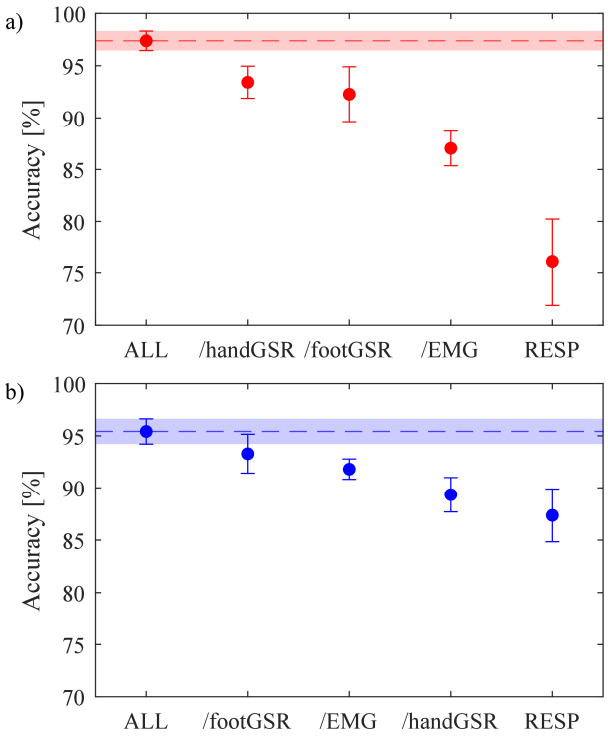

Fig. 2. Comparison of the accuracy of (a) cubic SVM and (b) fine KNN classifiers starting from a training performed with all the features and then removing, at each iteration, the indicated group and all the previous ones; for example, in the cubic SVM plot, /EMG at the fourth tick refers to a training performed with all the features except those related to the hand GSR, foot GSR and EMG signals.

classifier is related to its time advantage. In fact, since the KNN classifier does not require a real training step, large memories that allow to store all available data before starting the training step are needed [36]. Furthermore, as already pointed out, although simple and widely used, the KNN classifier does not maintain high performance when dealing with large datasets [31], [36].

IV. CONCLUSIONS

This work presented a method to assess stress level during driving in an objective way by using information from different physiological districts brought by several wearable physiological sensors. The process of feature extraction has a strong influence on the classification performance and consequently on the evaluation of the stress level. We compared our results with the ones obtained by other studies where different patterns of features were extracted on the same dataset, reporting an accuracy of 97% using all the signals [33] and an accuracy of 95.83% and 97% respectively when considering only the GSR signal or the EMG [34].

Therefore, our approach, also including data augmentation, proved its efficacy by reaching an accuracy of 98.4% when considering all features representative of different physiological responses. Feature analysis revealed how each physiological district may influence the classification performance, thereby identifying the most relevant ones. In addition, the use of a 60 heartbeat sliding window resulting in a larger dataset, allowed higher training performance and consequently a better prediction of the stress level. The comparison between the two classification algorithms in terms of relative accuracy and training time suggested that our approach could be possibly implemented for real time stress evaluation. The described approach

represents a promising tool for future studies on objective stress level detection not only during driving, but also in relation to other activities.

Despite the promising results obtained in this study, the feature selection step remains a supervised and time consuming approach and strongly affects the final outcome of the procedure for stress assessment. A more in-depth study on the role of features on performance could ensure an improved classification performance by reducing the classification time.

Our method is based on physiological data collected on drivers during different stress related activity; to extend the potentiality of our approach it would be meaningful to enlarge the range of the collected data to other activities and physiological districts. An unsupervised learning approach allowing a direct processing of raw physiological signals should be investigated in order to make the system suitable for real-time applications.

ACKNOWLEDGMENT

RP was supported by the Italian MIUR PON R&I 2014-2020 AIM project no. AIM1851228-2. LF was supported by the Italian MIUR PRIN 2017 project 2017WZFTZP "Stochastic forecasting in complex systems".

REFERENCES

[1] F.-X. Lesage, S. Berjot, and F. Deschamps, "Clinical stress assessment using a visual analogue scale," *Occup. Med. (Chic. Ill).*, vol. 62, no. 8, pp. 600–605, 2012.

[2] E.-H. Lee, "Review of the psychometric evidence of the perceived stress scale," *Asian Nurs. Res. (Korean. Soc. Nurs. Sci).*, vol. 6, no. 4, pp. 121–127, 2012.

[3] M. Zanetti *et al.*, "Assessment of mental stress through the analysis of physiological signals acquired from wearable devices," *Lect. Notes Electr. Eng.*, vol. 544, pp. 243–256, 2018, doi: 10.1007/978-3-030-05921-7_20.

[4] J. Huang, X. Luo, and X. Peng, "A novel classification method for a driver's cognitive stress level by transferring interbeat intervals of the ecg signal to pictures," *Sensors*, vol. 20, no. 5, p. 1340, 2020.

[5] S. Pourmohammadi and A. Maleki, "Stress detection using ECG and EMG signals: A comprehensive study," *Comput. Methods Programs Biomed.*, vol. 193, p. 105482, 2020.

[6] A. S. Anusha *et al.*, "Electrodermal activity based pre-surgery stress detection using a wrist wearable," *IEEE J. Biomed. Heal. informatics*, vol. 24, no. 1, pp. 92–100, 2019.

[7] J. W. Ahn, Y. Ku, and H. C. Kim, "A novel wearable EEG and ECG recording system for stress assessment," *Sensors*, vol. 19, no. 9, p. 1991, 2019.

[8] T. G. M. Vrijkotte, L. J. P. Van Doornen, and E. J. C. De Geus, "Effects of work stress on ambulatory blood pressure, heart rate, and heart rate variability," *Hypertension*, vol. 35, no. 4, pp. 880–886, 2000.

[9] R. Gupta, M. A. Alam, and P. Agarwal, "Modified Support Vector Machine for Detecting Stress Level Using EEG Signals," *Comput. Intell. Neurosci.*, vol. 2020, 2020, doi: 10.1155/2020/8860841.

[10] K. Soman, A. Sathiya, and N. Suganthi, "Classification of stress of automobile drivers using Radial Basis Function Kernel Support Vector Machine," *2014 Int. Conf. Inf. Commun. Embed. Syst. ICICES 2014*, no. 978, pp. 4–8, 2015, doi: 10.1109/ICICES.2014.7034000.

[11] T. Rahman, A. K. Ghosh, M. H. Shuvo, and M. Rahman, "Mental Stress Recognition using K-Nearest Neighbor (KNN) Classifier on EEG Signals," *Int. Conf. Mater. Electron. Inf. Eng. ICMEIE*, no. June 2015, pp. 1–4, 2015.

[12] S. Z. Bong, M. Murugappan, and S. Yaacob, "Analysis of electrocardiogram (ECG) signals for human emotional stress classification," *Commun. Comput. Inf. Sci.*, vol. 330 CCIS, no. September 2013, pp. 198–205, 2012, doi: 10.1007/978-3-642-35197-6_22.

[13] J. A. Healey and R. W. Picard, "Detecting stress during real-world driving tasks using physiological sensors," *IEEE Trans. Intell. Transp. Syst.*, vol. 6, no. 2, pp. 156–166, 2005.

[14] J. A. Healey, "Wearable and automotive systems for affect recognition from physiology." Massachusetts Institute of Technology, 2000.

[15] F. Shaffer and J. P. Ginsberg, "An overview of heart rate variability metrics and norms," *Front. public Heal.*, p. 258, 2017.

[16] M. A. F. da Silva, R. L. de Carvalho, and T. da Silva Almeida, "Evaluation of a Sliding Window mechanism as DataAugmentation over Emotion Detection on Speech," *Acad. J. Comput. Eng. Appl. Math.*, vol. 2, no. 1, pp. 11–18, 2021.

[17] J. Pan and W. J. Tompkins, "A real-time QRS detection algorithm," *IEEE Trans. Biomed. Eng.*, no. 3, pp. 230–236, 1985.

[18] L. R. Altimari, J. L. Dantas, M. Bigliassi, T. F. D. Kanthack, A. C. Moraes, and T. Abrão, "Influence of different strategies of treatment muscle contraction and relaxation phases on EMG signal processing and analysis during cyclic exercise," *Comput. Intell. Electromyogr. Anal. Perspect. Curr. Appl. Futur. challenges*, pp. 97–116, 2012.

[19] A. S. P. Sousa and J. M. R. S. Tavares, "Surface electromyographic amplitude normalization methods: a review," *Electromyogr. new Dev. Proced. Appl.*, 2012.

[20] M. A. C. Garcia and T. M. M. Vieira, "Surface electromyography: Why, when and how to use it," *Rev. andaluza Med. del Deport.*, vol. 4, no. 1, pp. 17–28, 2011.

[21] M. A. Oskoei and H. Hu, "Myoelectric control systems—A survey," *Biomed. Signal Process. Control*, vol. 2, no. 4, pp. 275–294, 2007.

[22] S. A. H. Aqajari, E. K. Naeini, M. A. Mehrabadi, S. Labbaf, A. M. Rahmani, and N. Dutt, "Gsr analysis for stress: Development and validation of an open source tool for noisy naturalistic gsr data," *arXiv Prepr. arXiv2005.01834*, 2020.

[23] A. Greco, G. Valenza, A. Lanata, E. P. Scilingo, and L. Citi, "cvxEDA: A convex optimization approach to electrodermal activity processing," *IEEE Trans. Biomed. Eng.*, vol. 63, no. 4, pp. 797–804, 2015.

[24] H. F. Posada-Quintero, J. P. Florian, A. D. Orjuela-Cañón, T. Aljama-Corrales, S. Charleston-Villalobos, and K. H. Chon, "Power spectral density analysis of electrodermal activity for sympathetic function assessment," *Ann. Biomed. Eng.*, vol. 44, no. 10, pp. 3124–3135, 2016.

[25] "Toolbox, Statistics and machine learning," 2017. .

[26] C. Cortes and V. Vapnik, "Support-vector networks," *Mach. Learn.*, vol. 20, no. 3, pp. 273–297, 1995.

[27] G. Guo, H. Wang, D. Bell, Y. Bi, and K. Greer, "KNN model-based approach in classification," in *OTM Confederated International Conferences" On the Move to Meaningful Internet Systems"*, 2003, pp. 986–996.

[28] D. Berrar, "Cross-Validation." 2019.

[29] B. G. Marcot and A. M. Hanea, "What is an optimal value of k in k-fold cross-validation in discrete Bayesian network analysis?," *Comput. Stat.*, vol. 36, no. 3, pp. 2009–2031, 2021.

[30] E. K. Garcia, S. Feldman, M. R. Gupta, and S. Srivastava, "Completely lazy learning," *IEEE Trans. Knowl. Data Eng.*, vol. 22, no. 9, pp. 1274–1285, 2009.

[31] D. Bzdok, M. Krzywinski, and N. Altman, "Machine learning: supervised methods," *Nat. Methods*, vol. 15, no. 1, p. 5, 2018.

[32] T. L. Prasanthi, "Machine Learning-based Signal Processing by Physiological Signals Detection of Stress," *Turkish J. Comput. Math. Educ.*, vol. 12, no. 11, pp. 4831–4840, 2021.

[33] M. Memar and A. Mokaribolhassan, "Stress level classification using statistical analysis of skin conductance signal while driving," *SN Appl. Sci.*, vol. 3, no. 1, pp. 1–9, 2021, doi: 10.1007/s42452-020-04134-7.

[34] O. Vargas-Lopez, C. A. Perez-Ramirez, M. Valtierra-Rodriguez, J. J. Yanez-Borjas, and J. P. Amezquita-Sanchez, "An explainable machine learning approach based on statistical indexes and svm for stress detection in automobile drivers using electromyographic signals," *Sensors*, vol. 21, no. 9, 2021, doi: 10.3390/s21093155.

[35] A. Limshuebchuey, R. Duangsoithong, and T. Windeatt, "Redundant feature identification and redundancy analysis for causal feature selection," in *2015 8th Biomedical Engineering International Conference (BMEiCON)*, 2015, pp. 1–5.

[36] J. Salvador–Meneses, Z. Ruiz–Chavez, and J. Garcia–Rodriguez, "Compressed kNN: K-nearest neighbors with data compression," *Entropy*, vol. 21, no. 3, p. 234, 2019.